X Rays and Electrons Emitted in Coincidence with the Fission of Cf^{252}†

R. A. ATNEOSEN* AND T. D. THOMAS‡
Frick Chemical Laboratory and Princeton-Pennsylvania Accelerator, Princeton University, Princeton, New Jersey

AND

WALTER M. GIBSON
Bell Telephone Laboratories, Murray Hill, New Jersey

AND

MORRIS L. PERLMAN
Chemistry Department, Brookhaven National Laboratory, Upton, New York

(Received 23 February 1966)

We have measured the emission times of K x rays and the yield and spectra of conversion electrons produced in coincidence with the spontaneous fission of Cf^{252}. The measurements of x-ray yield as a function of time since fission can be analyzed into components with half-lives of 2.4, 0.4, 0.05, and <0.01 nsec with relative numbers of nuclei 45, 25, 10, and 20, respectively. The yield of conversion electrons falls almost exponentially from 30 keV, the lowest energy measured, to about 500 keV; this falloff can be accounted for by the energy dependence of internal conversion coefficients. The yield of conversion electrons as a function of mass reaches a maximum at about mass 108, a minimum at mass 130, and a pronounced maximum at about mass 153. There is a sharp decrease in yield beyond this second maximum. The combination of x-ray half-lives and energies observed is consistent with low multipolarity transitions, mostly $M1$-$E2$ mixtures with some $E2$ and perhaps some $E1$. The gross features of the yield as a function of mass can be understood in terms of the stable nuclear deformations beyond mass 150, of postulated deformations for the neutron-rich nuclides near mass 108, and of the closed-shell properties of nuclides near mass 132. Various explanations for the sharp drop in yield beyond 153 are explored. It is suggested that the amount of spin acquired by a fragment at scission may depend critically on the partner fragment; spherical fragments are less effective at imparting spin to their partners than are deformed ones. This suggestion provides an explanation for the drop in electron yield at mass 153 and for some of the differences between the yield and spectrum of K x rays for Cf^{252} and these quantities for U^{236}.

I. INTRODUCTION

IN a very short time after fission the greater part of the excitation energy of the fragments is dissipated in neutron evaporation. About 8–10 MeV, however, are carried off by the emission of 8 to 10 gamma rays. Investigations of the gamma rays following fission have been directed toward understanding the de-excitation process itself and towards gaining information on the properties of the neutron-rich nuclides that are produced in fission.[1,2]

Data on the lifetimes and average energies of the transitions and on the angular distribution of the gamma rays with respect to the fission-fragment direction suggest that there is a large contribution from quadrupole radiation during de-excitation. This conclusion, together with the multiplicity of gamma rays (4 or 5 per fragment) indicates that the fragments are formed with rather high angular momentum—perhaps as much as 10 $\hbar$. Measurements of the multiplicity as a function of the mass of the fission fragment have given evidence for the existence of a new region of stable nuclear deformation for the neutron-rich nuclides of masses 90–110. This hypothesis has received support from measurements of the yield of K x rays in fission as a function of fragment mass.[3,4] The work of Thompson, Bowman, and their collaborators[4] shows promise of giving information on specific transitions in specific fission products.

In this work we have concentrated on a certain class of the transitions that de-excite fragments from the spontaneous fission of Cf^{252}, namely, those with low enough energy and high enough multipolarity that they are internally converted. For Cf^{252} the probability per fission of K x-ray emission is 0.57 (Refs. 3,4). In other words, about 6% of the radiations belong in this category. Two types of experiments have been done. We have measured the rate of K x-ray emission as a function of the time following fission for times up to 7 nsec and with time resolution as small as 0.2 nsec.

† This work supported in part by the U. S. Atomic Energy Commission.

* Present address: Department of Physics, Michigan State University, East Lansing, Michigan.

‡ Alfred P. Sloan Research Fellow, 1965-67.

[1] S. A. E. Johansson and P. Kleinheinz, in *Alpha-, Beta-, and Gamma-Ray Spectroscopy* edited by K. Siegbahn (North-Holland Publishing Company, Amsterdam, 1965), Vol. I, p. 805.

[2] H. Maier-Leibnitz, P. Armbruster, and H. J. Specht, in *Physics and Chemistry of Fission* (International Atomic Energy Agency, Vienna, 1965), Vol. II, p. 113.

[3] L. E. Glendenin and J. P. Unik, Phys. Rev. **140**, B1301 (1965); L. E. Glendenin, H. C. Griffin, and J. P. Unik, in *Physics and Chemistry of Fission* (International Atomic Energy Agency, Vienna, 1965) Vol. I, p. 369.

[4] S. S. Kapoor, H. R. Bowman, and S. G. Thompson, Phys. Rev. **140**, B1310 (1965); H. R. Bowman, S. G. Thompson, R. L. Watson, S. S. Kapoor, and J. O. Rasmussen, *Physics and Chemistry of Fission* (International Atomic Energy Agency, Vienna, 1965), Vol. II, p. 125; R. L. Watson, H. R. Bowman, S. G. Thompson, and J. O. Rassmussen, Phys. Rev. Letters **14**, 183 (1965).

The results of these measurements together with those obtained by other investigators[1–4] provide information on the multipolarities of the low-energy transitions. In addition, we have measured the yield and spectrum of conversion electrons emitted after fission as a function of fission-fragment mass. The yield data corroborate and extend the data obtained by others on the number of K x rays produced in fission as a function of mass.[3,4]

II. EXPERIMENTAL PROCEDURE

A. K X-Ray Measurements

The experimental method is based on the fact that the fission fragments have velocities of about 10^9 cm/sec. If an x-ray detector is so collimated that it can detect radiation from only those fragments that have moved a distance between d and $d+\Delta d$ cm from the source, it will detect only those x rays that are emitted between d and $d+\Delta d$ nsec after fission.

A schematic drawing of the apparatus is shown in Fig. 1. The californium source and a semiconductor fission-fragment detector were attached to a movable slide in an evacuated chamber. One wall of the chamber was a 2-in. lead block with a slot 1 cm wide cut in it. Directly above this slot was placed a sodium iodide crystal attached to a photomultiplier tube. The source could be positioned anywhere from a point directly under the collimating slot to a point about 6.5 cm back from the slot. The dimensions of the slot and of the semiconductor detector were such that any fission fragment that struck the detector must have passed under the collimator. This arrangement guaranteed that, to first order, the geometrical detection efficiency of the system did not depend on the source-to-collimator distance. Only x rays emitted when the fragment was opposite the slot could reach the scintillation detector.

Since the counting rate decreased rapidly as the distance between the source and collimator was increased, measurements were made with collimators of two different widths. At small distances, where the coincidence rate was high but changing rapidly, a brass sleeve with a 2-mm wide slot was inserted into the 1-cm opening so as to restrict the length of flight path viewed by the crystal to a few millimeters. This width gave the best time resolution possible consistent with a usable counting rate. At large source-to-collimator distances, where a higher coincidence rate was desired and good time resolution was not needed, data were obtained with the brass sleeve removed. In this case, the collimator walls were lined with a graded absorber constructed of 0.032-in. cadmium, 0.016-in. copper, and 0.01-in. aluminum. This absorber removed x rays with energies in the region of interest due to fluorescence along the walls of the collimator initiated by fission fragments and post-fission gamma rays. The net aperture was then about 7 mm wide.

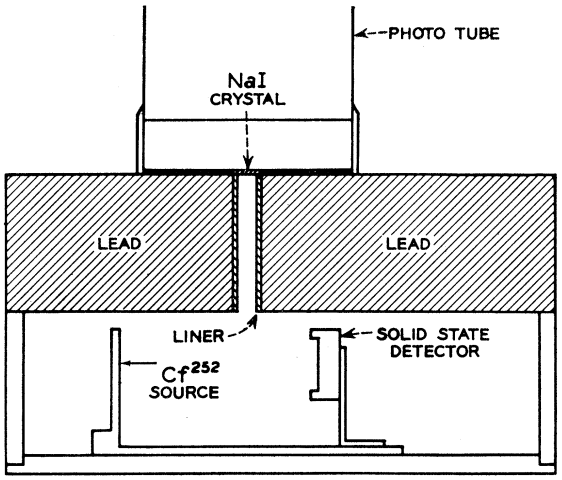

FIG. 1. Schematic drawing of apparatus used to determine emission times of K x rays.

The fission-fragment detector was a 300-mm² surface-barrier detector. The scintillation crystal used with the 2-mm slot was 2 mm wide, 5 cm long, and 1 mm thick; that used with the 7-mm slot had the same depth and length but was 10 mm wide. These dimensions were chosen so as to minimize the sensitivity of the detector to high-energy gamma rays and neutrons. Both crystals were integrally mounted NaI(Tl) units with resolutions of about 45% at 6 keV.

The source for these measurements was prepared by electrodeposition of californium from an ammonium sulfate solution onto a nickel foil, 100 μg/cm² thick, backed by 2 mg/cm² of copper. The deposit was covered with an additional 50 μg/cm² thick nickel foil to inhibit loss of material from the source.

The fission-fragment and x-ray detector signals were amplified in conventional preamplifiers and double-delay-line clipped linear amplifiers. The output pulses from the two amplifiers were fed to a multiple coincidence unit set for a resolving time of about 130 nsec. The pulses from the x-ray detection system were also analyzed by multichannel pulse-height analyzer, which was gated by the coincidence output.

Two measurements were made at each source-to-collimator distance. One was made with no absorber between the sodium iodide crystal and the chamber other than the necessary thin aluminum windows (a total of 31 mg/cm²). The other was made with copper (0.4 g/cm²) and aluminum (0.2 g/cm²) absorbers covering the entrance to the collimator. The transmission of this absorber for 50-keV photons was calculated to be 31%. The absorber was essentially opaque for x rays of interest (20 to 40 keV) and practically transparent for higher energy photons.[5] The spectra measured with the absorber in place represent the background due to high-energy photons and other radiations in coinci-

[5] G. W. Grodstein, Natl. Bur. Std. Circ. No. 583, (1957).

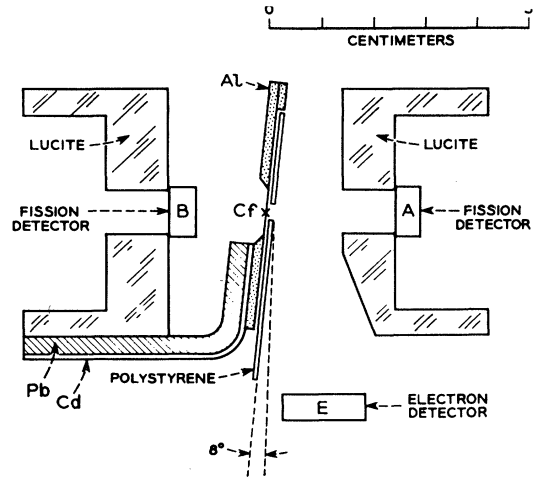

FIG. 2. Schematic drawing of apparatus used to determine spectra of conversion electrons as a function of fission fragment mass.

dence with fission that deposited a small fraction of their energy in the crystal. The difference between the two spectra yields to good approximation the spectrum of low-energy photons in coincidence with fission.

B. Electron Measurements

The arrangement used in the electron experiment is represented schematically in Fig. 2. A source of Cf^{252} yielding about 5×10^5 fissions per minute was sandwiched between two nickel foils, 50 and 100 $\mu g/cm^2$ thick. Semiconductor detectors, A and B, were placed on opposite sides of the source to detect fission fragments in coincidence with an event in electron detector E, which was positioned so as to accept radiations emitted from the fragments at approximately 90° to their direction of motion. The configuration used was such that electrons were detected from only the fragment directed towards detector A (the other fragment then being detected in B). To achieve this purpose, a $\frac{1}{32}$-in. thick sheet of polystyrene with a $\frac{1}{8}\times\frac{1}{8}$ in. hole in it was placed $\frac{1}{32}$ in. away from the surface of the californium source on the same side as detector A, and the source was set so that the normal to its plane made an angle of 8° with the line between detectors A and B. Also, the electron detector was shielded from each fission detector to prevent the detection of electrons from the stopped fragments. With this arrangement, only those electrons could be detected that were emitted at positions between 0.1 and 1.5 cm along the flight path of the fragment eventually detected in A. It was thus possible to identify which of the two fragments emitted the electron. The polystyrene sheet served also to reduce greatly the number of alpha particles and fission fragments striking the electron detector.

Since the electron detector was partially sensitive to low-energy gamma rays, a $\frac{1}{4}$-in. thick lead absorber covered with $\frac{1}{32}$-in. thick cadmium was placed so as to absorb gamma rays emitted from fission fragments traveling towards detector B. The cadmium served to remove the lead K x rays caused by fluorescence as these had energies in the range of interest. However, the background was still quite high since most of the gamma rays were emitted by fragments close to the source and these could not be removed without blocking out particles of interest.

All surfaces close to the electron detector and source were covered with polystyrene or Lucite to reduce the probability for observing scattered electrons, which would be degraded in energy. However, the polystyrene sheet over the source was covered with 0.00045-in. thick aluminum foil grounded to the source holder to guard against the possible rupture of the nickel foils from electrostatic charging of the plastic.

The fission fragments were detected with diffused-junction semiconductor detectors subtending angles of 24° (detector A) and 41° (detector B). Detector B intercepted 90 to 95% of the partners of fragments incident on A. It was necessary to replace these detectors several times during the experiment because of deterioration caused by fission fragments. A silicon surface-barrier detector with a depletion depth of about 1 mm and an area of 200 mm^2 was used as the electron detector; it was placed 3.6 cm from the path between the source and detector A and subtended an angle of 25.4° (1.24% of 4π) at a point a few millimeters from the californium source in the direction of A. This geometrical efficiency was determined by measurements with a calibrated alpha-particle source and was also calculated from the dimensions. The electron detector was cooled to dry-ice temperatures. Measurements with Cs^{137} and Hg^{203}, also used for the energy calibration, indicated that the resolution of the electron detection system was 14 keV full width at half-maximum. Reliable information could be obtained for electrons with energies as low as 35 to 40 keV.

Conventional preamplifiers and amplifiers were used with the fission detectors. The electron pulses were amplified with a low-noise ORTEC 103-203 system. In order to minimize problems due to the overload pulses that occurred when fission fragments or alpha particles struck the electron detector, diode-limiting circuits were incorporated in the preamplifier and amplifier for the electron detector. Even with the limiters, the amplifier did not return to its quiescent state for about 60 μsec after a fission pulse. A discriminator circuit was therefore used to generate a signal that prevented the coincidence circuit from producing a gating pulse for 60 μsec after such an overload pulse. With the polystyrene baffle, the number of fission fragments and alpha particles detected in the electron detector was very low, being about 20 and 300/min, respectively. These events are thought to have originated from the diffuse edge of the source and from a small amount of californium contamination in the chamber. The fraction of the time for which the coincidence gate was

blocked was about 1%; most of the blocking pulses were initiated by higher energy electrons for which the amplifier returned to its quiescent state in a time much less than 60 μsec.

The outputs of the three amplifiers were fed to a triple coincidence unit with resolving time of about 1 μsec. This large resolving time was dictated by the requirement of full coincidence efficiency with the lowest energy electron pulses, for which the time jitter of the crossover point caused by electronic noise was appreciable. The resulting chance rate was 5% of the total coincidence rate.

The amplified pulse heights, X_A and X_B, from the two fission detectors, A and B, were fed to an adder-divider circuit[6] that generated a pulse proportional to $X_B/(X_A+X_B)$. Because the pulse-height defect depends approximately linearly on the fragment mass,[7–9] the pulse-height ratio is linearly related to the kinetic-energy ratio, $E_B/(E_A+E_B)$, where E_A and E_B are the kinetic energies of the two fragments. It follows from conservation of momentum that, if no neutrons are emitted from the fragments, this energy ratio is equal to the mass ratio, $M_A/(M_A+M_B)$, where M_A and M_B are the masses of the two fragments and M_A+M_B is, in this case, 252. Except for a small correction due to neutron emission, the pulse from the adder-divider circuit is therefore linearly dependent on the primary mass of the fragment detected in counter A.

Measurements with a calibrated pulser and pulse-height analyzer showed that the ratio of the output of the divider circuit to that calculated from the known inputs was constant to within 2% over the range of interest for fission fragments. The peak-to-valley ratio for the mass distribution for binary fission was about 10 to 1. Further consideration of the accuracy of this method of mass measurement is presented in the Appendix.

The output of the divider circuit and the output from the amplifier in the electron detector circuit were used as the two inputs of a two-parameter pulse-height analyzer, which was gated by the coincidence circuit. The data stored in the analyzer thus represented the electron spectrum as a function of the mass of the fragment emitting the electron.

The data were stored in a 64×64 channel array. Because of the small number of channels on the electron-energy axis, it was necessary to make two sets of measurements, one for the energy range from 40 to 300 keV and the other for the range from 300 to 650 keV. For each set of measurements the background due to gamma rays in coincidence with fission was measured as a function of fragment mass with a $\frac{1}{8}$-in. thick polystyrene absorber over the electron detector. This absorber stopped electrons of energy up to about 800 keV but had a negligible effect on gamma rays. The difference between the spectra taken with and without the absorber represents the electron spectrum. The background accounted for two-thirds of the total coincidence rate.

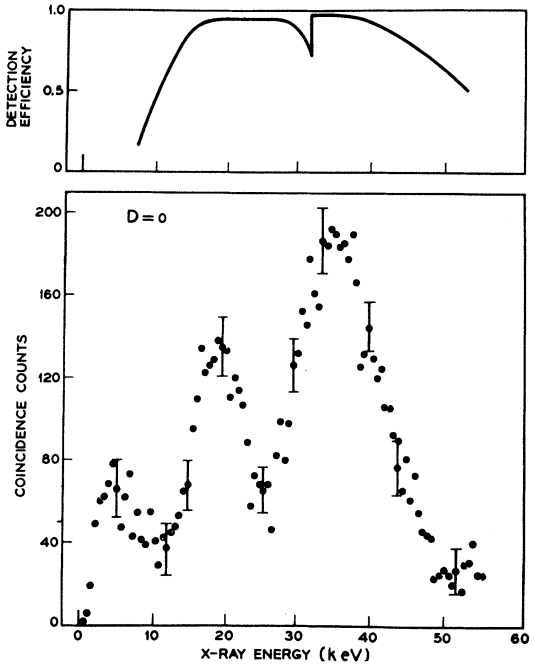

FIG. 3. Lower part: Spectrum of x rays emitted from fission fragments within about 7 mm of the source position. Upper part: Efficiency of the x-ray detector.

The low net coincidence rate of about 10 counts per minute and the high associated background rate meant that a long period of time was required to obtain statistically meaningful data. During this time, adjustments were made to compensate for drifts. These were especially important for the fission detectors, whose response steadily deteriorated. Every few days, the accumulated data were transferred to punched paper tape, and the outputs of both fission detectors, the divider circuit, and the electron detector were compared with standard spectra previously stored on tape. Also, the zero levels on each side of the analyzer, discriminator levels, etc. were checked. After the necessary (but usually small) adjustments were made, the accumulated data were read back into the analyzer and new data were added. In order to determine the electron yield per fragment as accurately as possible, mass measurements were made just before and just after each set of electron measurements.

[6] G. L. Miller and E. A. Gere, *IEEE Trans. Nucl. Sci.* **NS-11**, 382 (1964).

[7] H. W. Schmitt, W. M. Gibson, J. H. Neiler, F. J. Walter, and T. D. Thomas, in *Physics and Chemistry of Fission* (International Atomic Energy Agency, Vienna, 1965), Vol. I, p. 531.

[8] W. E. Stein, in *Physics and Chemistry of Fission* (International Atomic Energy Agency, Vienna, 1965), Vol. I. p. 491.

[9] T. D. Thomas, W. M. Gibson, and G. J. Safford, in *Physics and Chemistry of Fission* (International Atomic Energy Agency, Vienna, 1965), Vol. I, p. 467.

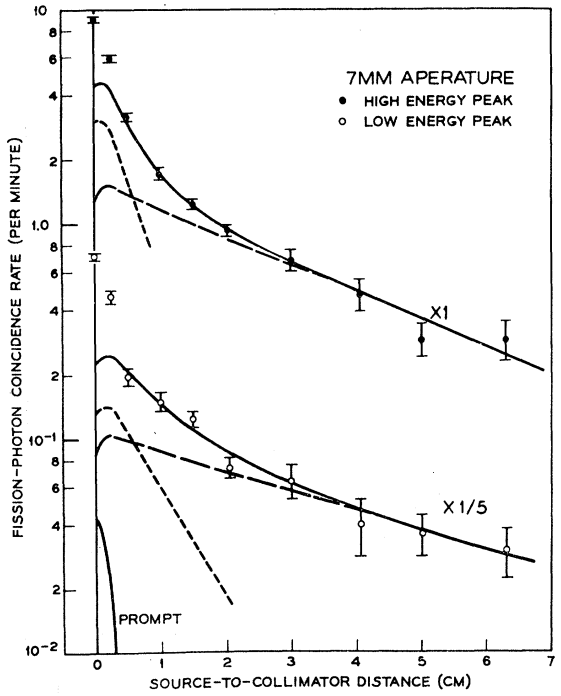

FIG. 4. Fission-photon coincidence rate as a function of source-to-collimator distance for the 7-mm collimator. The dashed curves represent a decomposition into exponentially decaying components. The upper solid curves represent their sums.

III. ANALYSIS AND RESULTS

A. X-Ray Measurements

The lower half of Fig. 3 shows the spectrum of photons observed in the x-ray detector, obtained with the source at zero distance from the 7-mm wide collimator. Background (see Sec. II) has been subtracted. At the "zero" position the source was directly below one edge of the collimator; thus the spectrum shown represents an integral of x-ray emissions occurring during approximately the first 7 mm of flight or, roughly, the first 0.7 nsec. The two major peaks, at about 20 and 35 keV, are due to K x rays from the light and heavy fission fragments, respectively. A similar spectrum was obtained with the 2-mm wide collimator.

The curve shown in the top half of Fig. 3 gives the fraction of x rays emitted into the collimator aperture detected in the scintillation crystal, calculated from standard absorption tables.[5] Three factors are important in determining the shape of this curve: attenuation in the window (responsible for the falloff at low energies), efficiency of the crystal for detecting x rays (seen mainly as the absorption edge at 33 keV and part of the falloff at higher energies), and excess subtraction of background at the high-energy end because of x rays transmitted through the absorber (causing a major portion of the attenuation there). Over the two x-ray peaks of interest the total efficiency is nearly unity. Integrating the reciprocal of this curve over each x-ray peak, one finds that the total counts in the light and heavy peaks should be increased by 21 and 15%, respectively. Unaccounted for in this heavy-peak correction is the loss in counts due to escape of iodine K x rays from the crystal. The escape peak should appear in the spectrum at about 5 to 10 keV. The x-ray spectrum of Fig. 3 shows evidence for a peak in this energy range, which, because of the large attenuation below 10 keV by the chamber window, is likely to be the escape peak. The counts below 10 keV correspond to 15% of the x rays above 33 keV. This number is somewhat smaller than expected, since the percent of escape from an even thicker crystal[10] is about 20%. Using our measured result of 15% and assuming the same attenuation for the escape peak as for the heavy peak, we find the light and heavy peaks should be increased 21 and 35%, respectively.

Summing counts in the light- and heavy-fragment peaks separately and applying the above corrections gives the total coincidence rate for each as a function of the source-to-collimator distance, as shown in Fig. 4. The rate for the light-fragment peak has been divided by 5 before plotting. These rates are based on a fixed (arbitrary) rate of 11 500/min in the fission-fragment detector. The "prompt" curve represents results of measurements of the rate of coincidences between the Cf^{252} alpha particles and curium L x rays emitted following the alpha decay of Cf^{252}. As such, it indicates the deviation from ideal geometry with a point source and point detector, for which the counting rate of prompt radiation would drop abruptly to zero as the source is moved behind the edge of the collimator. This deviation will be referred to here as an edge effect. The abscissa of Fig. 4 is the source-to-collimator distance rather than time since the transformation is complicated, especially for very short lifetimes and small source-to-collimator distances.

The obvious conclusion to be drawn from the data in Fig. 4 is that a large percentage of the radiation occurs at distances greater than a few millimeters and that the decay curve is complex, consisting of at least several components. In order to make a rough determination of the lifetimes and intensities, we have analyzed the data in terms of two or three simple exponential decays. For this analysis, it was convenient to determine the half-distances (the distance in which the intensity decreases by a factor of 2) rather than the corresponding half-lives. A least-squares fit of a simple exponential was made to the three or four points at the greatest distances to determine the half-distance of the longest lived component. The expected shape for a component with this half-distance was found by integrating an exponential decay rate over the experimental geometry for each source-to-collimator distance. The solid angle was taken to be constant for

[10] J. H. Neiler and P. R. Bell, in *Alpha-, Beta-, and Gamma-Ray Spectroscopy*, edited by K. Siegbahn (North-Holland Publishing Company, Amsterdam, 1965), Vol. I, p. 245.

fission fragments directly under the slot and to decrease to zero beyond the collimator with a cosine dependence chosen to match the prompt curve. The calculated curve was then normalized on the basis of the parameters obtained from the least-squares fit to the large-distance data. The results are shown as large-dash curves in Fig. 4 and correspond to half-distances of 2.3 cm (heavy fragment) and 3.3 cm (light fragment) with relative numbers of nuclei of 5.6 and 2.5, respectively. The initial increase in rate at small distances is a consequence of edge effects, since with the source a few millimeters back from the collimator edge, a slightly greater length of fragment flight path can be viewed by the crystal than when the source is exactly at the edge.

After the above components were subtracted from the data points, the same procedures were applied again giving the small-dash curves in Fig. 4. The corresponding heavy- and light-fragment components have half-distances of 0.34 and 0.61 cm with relative numbers of nuclei of 3.5 and 1.1, respectively. It is to be noted that although the collimator width is 0.7 cm, even shorter half-distances can be accurately determined.

Combining the two components determined in each case results in the solid curves of Fig. 4. These curves account for the x-ray rates at distances from 0.5 to 6.3 cm, but the points at 0.0 and 0.25 cm are considerably above the solid curves. They are considered to be associated with radiation with half-distances much less than 0.5 cm. The differences between these points and the solid curves are found to fall off at essentially the same rate as the prompt curve does. In each case, the difference in magnitude between the data point and the solid curve at zero distance is a measure of the total number of nuclei with very short lifetimes since it represents an integral over at least several half-lives.

The measurement of x-ray rates with the 7-mm wide collimator demonstrates the existence of very short-lived activity with sufficient intensity to be measured with improved resolution. Consequently, a series of measurements was made at small distances with a 2-mm wide collimator. The results are plotted in Fig. 5, where the heavy-fragment data have been increased by a factor of 5 before plotting. The corrections discussed for the 7-mm slot have been made and are the same except for the escape peak correction, which is 17%, somewhat larger as expected for the smaller crystal. To determine what part of the rates is due to the previously measured components, a composition of the two simple exponential decays for the heavy- and light-fragment x rays with half-distances and relative intensities as determined with the 7-mm wide collimator was integrated over the experimental geometry of the 2-mm wide collimator for all source-to-collimator distances. The shapes of the resulting curves agree nicely with the data points from 0.4 to 1.8 cm, as they should. These curves were then normalized to the data points from

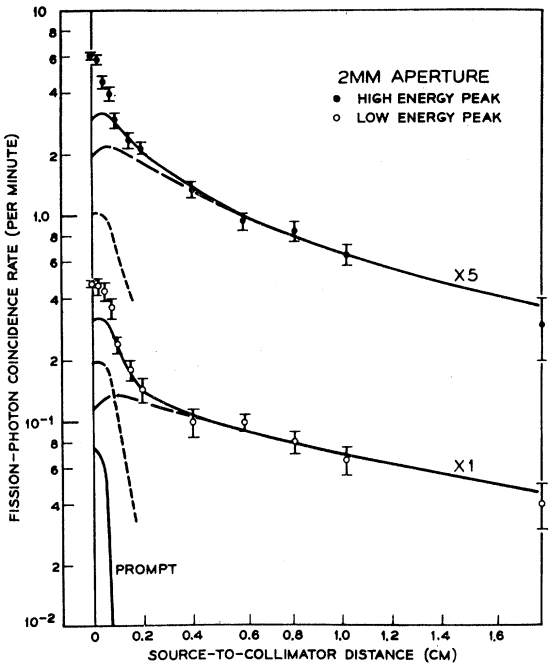

FIG. 5. Fission-photon coincidence rate as a function of source-to-collimator distance for the 2-mm collimator. The long-dashed curves are determined from the solid curves in Fig. 4. Addition of exponential decays shown by short-dashed curves yields the solid curves passing through the data points.

0.4 to 1.0 cm and are plotted as large-dash curves in Fig. 5. The normalization factors are in approximate agreement with the ratio of the geometrical factors. For both the heavy- and light-fragment x rays, the data points rise above the curve in the region from 0.1 to 0.2 cm, which is well outside of the prompt region.

Subtracting the longer lived components and applying the same analysis as before leads to the small-dash curves shown in the figure, which have half-distances of 0.07 cm and 0.04 cm for the heavy- and light-fragment radiations, respectively. Adding these components to the corresponding large-dash curves yields the solid curves, which fit the data quite well for distances of 0.1 cm and greater. Again there remains a measurable amount of short-lived radiation, which is found to fall off in the same way that the prompt radiation does. As before, the total number of nuclei with very short lifetimes is the difference between the measured rate and the solid curve at zero distance.

Detailed considerations of the experimental geometry show that the prompt radiation determined by the above procedure is overestimated since it includes some x rays emitted from partners of the fragments detected in the fission-fragment detector. These partners pass through the back of the source foil and can be viewed for only a very short time before the source-mounting frame becomes interposed between them and the x-ray crystal and only for source-to-collimator distances within the range of the prompt curve.

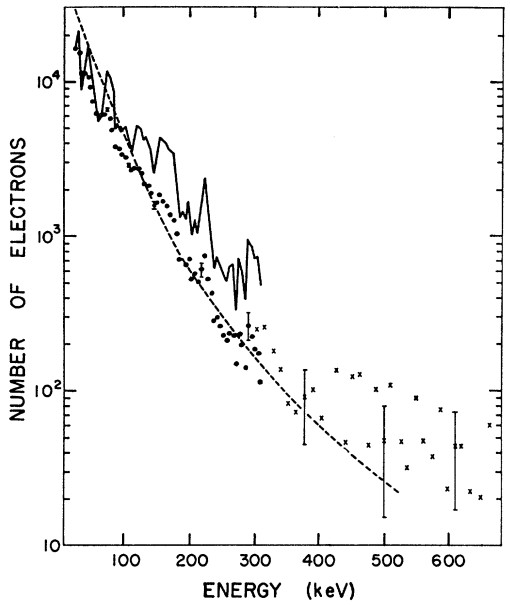

FIG. 6. Spectrum of electrons detected in coincidence with fission fragments between 0.1 and 1.5 cm from the source, summed over all fission fragment masses Points and crosses are the experimental data. The solid line represents the results of a correction for 76% backscattering from the electron detector. The dashed curve is calculated assuming a flat transition spectrum from 0 to 500 keV and equal probability for $E2$ and $M1$ transitions. Statistical errors are indicated for several points.

The tabulation of the results, corrected for the above-mentioned effect, obtained with both collimators is presented in Table I. Half-distances have been converted to half-lives using reported values of 1.036 and 1.375 cm/nsec for the average velocities of the heavy and light fragments, respectively.[11] The relative intensities measured with the two collimators are in good agreement for the heavy fragments. Some discrepancy is apparent for the relative intensities of the light-fragment radiations. There is evidence that the amount of prompt radiation measured for the light fragment with the 2-mm wide collimator is too low and the relative amounts of the other components thus too high. The alignment of the source and collimator planes for this aperture is quite critical and an appreciable fraction of the prompt low-energy x rays emitted by the detected fragment may have been absorbed by the nickel foils between which the source was deposited.

The results obtained for the K x-ray coincidence rates depend on the background corrections. With the 7-mm wide collimator, the background at zero distance represented about 20% of the counting rate; for the largest distances the background was as much as 60% of the rate. The corresponding background rates for the 2-mm wide collimator were 40 and 75%, respectively. The data collected at large distances are thus the most strongly influenced by errors in the background.

[11] S. L. Whetstone, Jr., Phys. Rev. **131**, 1232 (1963).

TABLE I. Relative number of atoms emitting K x rays with indicated half-distances and half-lives.

	$D_{1/2}$ (cm)	$T_{1/2}$ (nsec)	2-mm collimator intensity	7-mm collimator intensity
Heavy fragment	2.3	2.3	45	46
	0.34	0.33	28	29
	0.07	0.07	9	} 25
	zero	<0.01	18	
Light fragment	3.3	2.4	52	44
	0.61	0.44	22	19
	0.04	0.03	14	} 37
	zero	<0.01	11	

An important source of such error results from the deviation of the attenuation curve of the x-ray absorber from a sharp cutoff. This effect has been partially taken into account. Another possible source of background is electrons emitted by fission fragments. The chamber and x-ray detector windows stopped electrons below about 160 keV, and our electron data show that most of the fission electrons are of lower energy. The windows stopped also Compton electrons generated in the absorber since the majority of these were of low energy.

The work of Glendenin and Griffin[12] shows the existence of long-lived components with half-lives of 30 and 100 nsec and relative intensities of 7 and 8%, respectively. The 30-nsec component was found to be associated primarily with the light fragment. Since this component would have the greatest influence on our results, we have calculated the rate expected for it with our geometry in terms of our longest lived component (2.3 nsec) for the light-fragment peak. At zero distance, we conclude that the contribution of the 30-nsec component amounts to about 6% and at 6 cm it contributes about 18%. Because in our analysis we have neglected the presence of the 30- and 100-nsec components, the half-lives and intensities listed in Table I for the longest lived components are a little high. The effect on the shorter lived components is small.

The data shown in Table I indicate that the decay curves for light and heavy fragments are quite similar, especially if the discrepancy between the 2-mm and 7-mm results for the light fragments is corrected for. These results may be summarized by stating that there are components with half-lives of 2.4, 0.4, 0.05, and less than 0.01 nsec with relative numbers of nuclei 45, 25, 10, and 20, respectively. Only those nuclei decaying by internal conversion are included in these numbers. To the extent that there is correlation between half-life and internal conversion coefficient these numbers must be approximately adjusted.

It should be noted that the analysis into several components made here is not unique. It is likely that there are many more than the few lifetimes indicated contributing to the decay curves and that a continuous

[12] L. E. Glendenin and H. C. Griffin, Phys. Letters **15**, 153 (1965).

distribution of half-lives is a more accurate representation of the true situation. The half-lives and abundances we report here may be taken as averages over regions of this distribution. Furthermore, it is possible that the decay does not follow the first-order rate law that has been assumed here. The nuclear levels that undergo conversion are probably formed at the end of the de-excitation process and the radiation from them should follow a complicated growth and decay relationship. If the precursor half-lives are sufficiently short, however, this relationship will indeed be first order on the time scale studied here. The data of Johannson[13] indicate that most of the gamma rays are emitted with lifetimes of the order of a few times 10^{-11} sec, or at least a factor of 10 shorter than those of 70% of the converted transitions.

Comparison of the above results can be made with data obtained by others. The mean energies of the x rays associated with the heavy and light fragments in our experiments are about 35 and 19 keV, respectively, which are basically in agreement with, but slightly higher than, the values reported by Glendenin and Griffin.[12] Our value of 0.64 for the average yield of K x rays per fission is slightly higher than the values between 0.55 and 0.57 that have been reported.[3,4,12] We find, as did Glendenin and Griffin, that the heavy-fragment group corresponds to 70% of the total; Kapoor, Bowman, and Thompson,[4] measuring over the first 50 nsec after fission, report a value of 57% for the heavy-fragment group. Integrating over the components resulting from our simplified analysis and over the contributions from the two long-lived components reported by Glendenin and Griffin, we conclude that 29% of the x rays are emitted in the first 0.1 nsec, 27% between 0.1 and 1.0 nsec, 29% from 1 to 10 nsec, and 15% after 10 nsec. These results are well within experimental error of the corresponding values of 30, 30, 25, and 15% reported by Glendenin and Griffin. There is, however, some discrepancy between our results and those obtained by Kapoor, Bowman, and Thomspon by a more indirect method: 20% within 0.1 nsec, 57% between 0.1 and 1 nsec, and 23% between 1 and 50 nsec.

B. Electron Measurements

Displayed in Fig. 6 is the spectrum of electrons in coincidence with the fission of Cf^{252} after background and chance coincidence subtraction. The number of electrons per energy channel decreases almost exponentially with increasing electron energy so that, roughly, 95% of all those observed above the lower level discriminator (25 keV) are found to have energies less than 300 keV. The spectrum is fairly smooth, indicating that the various transitions are closely spaced on the average.

The shape of this spectrum and those shown in the following graphs are somewhat distorted because of backscattering of electrons from the solid-state detector. For example, measurements by Charoenkwan[14] of the 625-keV conversion-electron line from Cs^{137} show the presence of a flat tail extending from the main peak down to low energies. The height of this tail amounts to about 6% of the main peak height and corresponds to a backscattering coefficient (the number of backscattered electrons/number of incident primary electrons) of 37%. Measurements we have made with Xe^{131m} indicate that this coefficient is 76% for electrons of about 150 keV. Theoretically, the fraction of the incident electrons backscattered is independent of the energy of the incident electron[15]; the results just mentioned may contradict this idea, although it should be noted that the result of 37% reported by Charoenkwan and that of 76% found by us were obtained with different crystals in different geometries. Assuming that the backscattering coefficient is independent of energy and using a method similar to that outlined by Charoenkwan we have corrected the data of Fig. 6 for this effect. The solid curve of Fig. 6 represents the results of this correc-

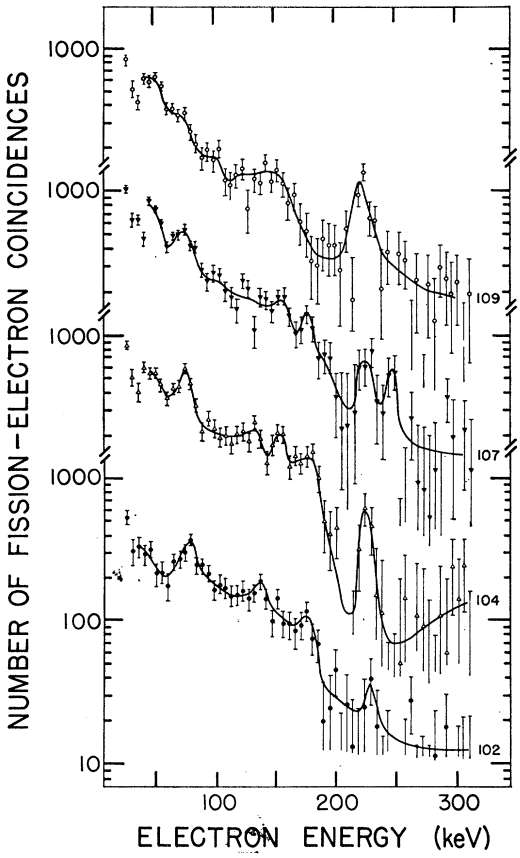

FIG. 7. Spectra of electrons detected in coincidence with light fission fragments between 0.1 and 1.5 cm from the source for the fragment masses indicated on the right. The mass intervals are about 2.5 mass units wide. Masses are after neutron emission.

[13] S. A. E. Johansson, Nucl. Phys. **60**, 378 (1964).

[14] P. Charoenkwan, Nucl. Instr. Methods **34**, 93 (1965).

[15] W. Bothe, Z. Naturforsch. **4a**, 542 (1949).

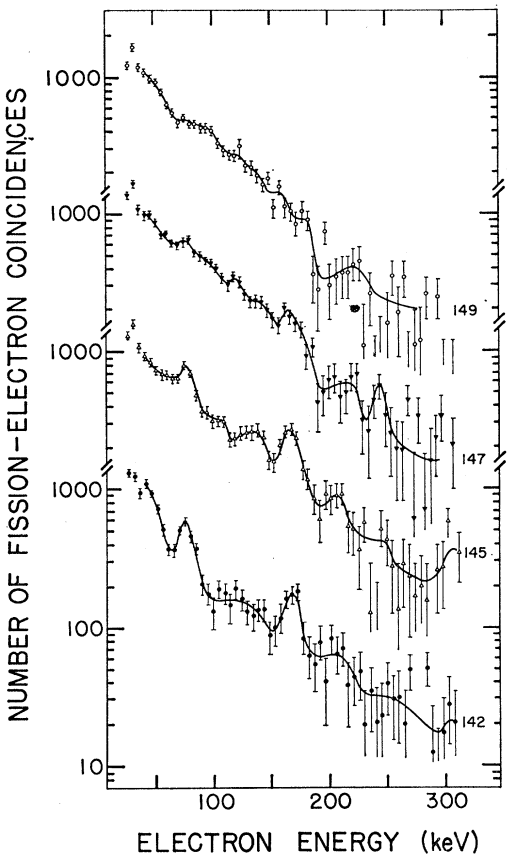

FIG. 8. Spectra of electrons detected in coincidence with heavy fission fragments between 0.1 and 1.5 cm from the source for the fragment masses indicated on the right. The mass intervals are about 2.5 mass units wide. Masses are after neutron emission.

tion procedure assuming a backscattering coefficient of 76%; the results with a coefficient of 37% are similar, but the fluctuations are less pronounced. In either case, the general exponential falloff of the number of events with increasing electron energy that is apparent in the original data is also present in the corrected data. The correction increases the total number of events under the curve by 50% for 76% backscattering and by 20% for 37% backscattering. This result is due to inclusion in the energy range of the curve of backscattered electrons depositing less than 25 keV in the detector.

In Figs. 7, 8, and 9, coincidence electron spectra (corrected for chance and background events) are displayed for several different mass groups. The spectra are labeled according to the average final mass of the fission fragment but have not been corrected for either backscattering or mass dispersion. The separation between mass channels, about 2.3 mass units, corresponds to the resolution (rms deviation) of the mass identification system. The first of these figures shows the spectra over the region of the light-fragment peak. Since, as will be seen, the number of electrons emitted per fragment is low in this region, statistical counting errors are large. A solid line has been drawn through the data in a way consistent with the error bars; some of the peaks indicated by the line may not be real. Since our net mass resolution is on the order of 2.3 units (rms), any real peak should appear in at least two adjacent spectra. Considerable structure is apparent at all masses and there seem to be so many transitions that much of the structure is unresolved. A fairly strong line extending over several mass units occurs at about 75 keV. Another line can be resolved at 225 keV in the mass-104 spectrum. The data below about 40 keV are considered to be unreliable because of possible variations in the noise level or discriminator setting during runs. Furthermore in the energy range below 40 keV there are contributions from Auger electrons.

Figures 8 and 9 show the coincidence electron spectra in the region of the heavy-mass peak; the first of these, starting at the bottom, displays the spectra going up the light side and slightly over the top of the heavy peak while the second, beginning at the top, gives the spectra going down the upper side of the heavy peak. A maximum in the electron yield occurs at a slightly greater mass than that of the most probable heavy fragment. The general features of these spectra are

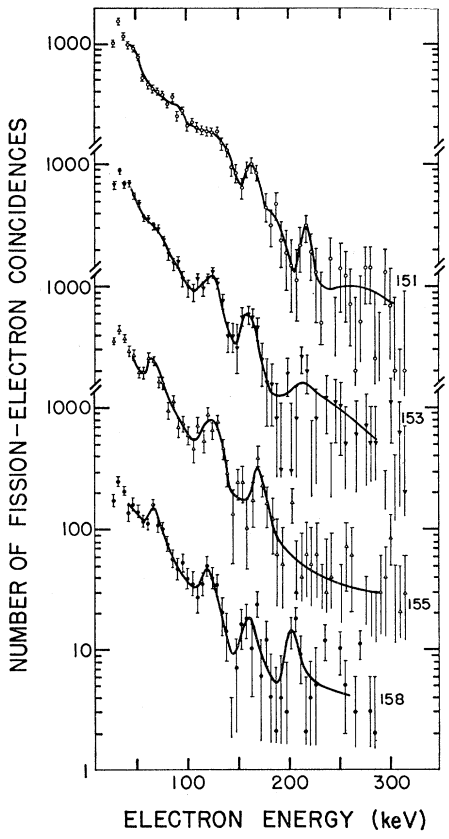

FIG. 9. Spectra of electrons detected in coincidence with heavy fission fragments between 0.1 and 1.5 cm from the source for the fragment masses indicated on the right. The mass intervals are 2.5 mass units wide. Masses are after neutron emission.

quite similar to those associated with the light fragments. For the curves away from those representing the maximum electron yield several transitions can be resolved in each spectrum. However, in the region of the maximum yield, the number of transitions increases to a point at which no lines can be resolved below 150 keV and only a few at higher energies.

From the sum over the electron spectrum at each mass and the mass yield curve, we obtain the number of electrons emitted per fragment as a function of fragment mass. The uncorrected yields over the energy range 40 to 70 keV obtained from three consecutive measurements of electrons plus gamma rays (solid symbols) and of gamma rays along (open symbols) are plotted in Fig. 10. This graph is intended to show the general reproducibility of the data and of the features of interest. The scatter of the data points results mostly from statistical counting errors. The contribution of gamma-ray background amounts to only 33% of the total around mass 155, 60% around mass 110, and it approaches 100% at symmetry.

Figure 11 shows the number of electrons per fragment as a function of final mass for several ranges of electron energy. To obtain these curves we have corrected the original data for chance events and for mass dispersion ($\sigma=2.3$ mass units) and have taken the ratio at each mass of the rate of triple coincidences (electron-fission A-fission B) to the rate of double coincidences (fission A-fission B). The difference between ratios from data taken without and with an electron absorber gives the relative number of electrons per fragment. This quantity corrected for the geometric efficiency of the electron detector is approximately the absolute number of electrons per fragment. Results for the region of symmetric fission (mass 124) have been omitted because of the small number of electrons relative to the gamma-ray background and the high sensitivity to small shifts in the yield curve there. Details of the mass-dispersion correction and the mass calibration are given in the Appendix.

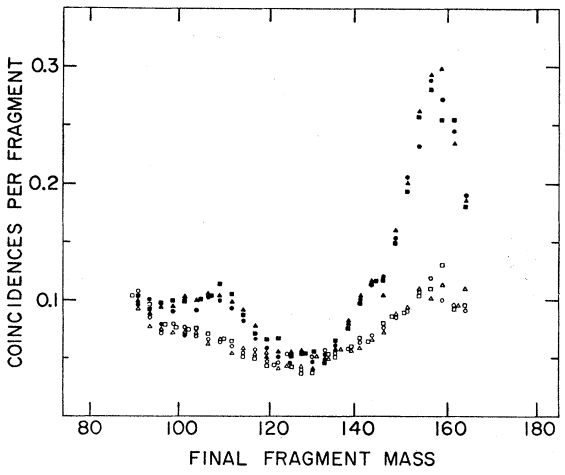

FIG. 10. Coincidences between the electron detector and the fission detectors per fission fragment as a function of fragment mass. Three successive runs are shown as triangles, circles, and squares. Solid points represent the sum of electrons and gamma rays. Open points represent the gamma-ray background.

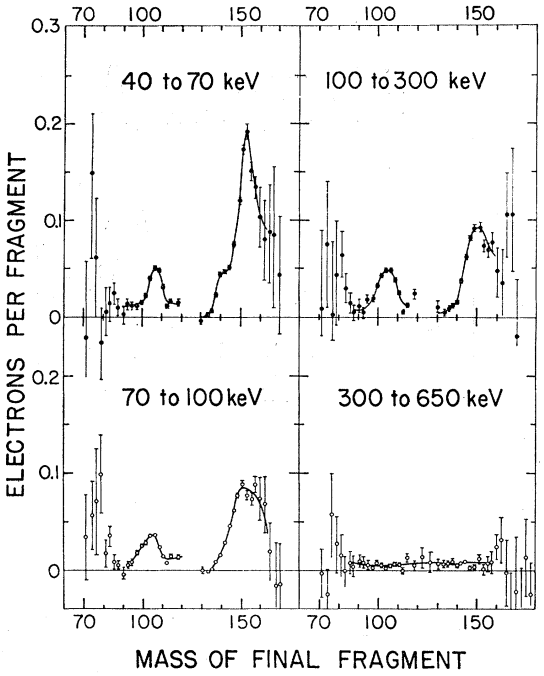

FIG. 11. Yield of electrons from fission fragments between 0.1 and 1.5 cm from the source as a function of final fragment mass for selected electron-energy intervals.

The electron yields per fragment shown in Fig. 11 are lower than the true yields. No corrections for backscattering have been made; on the basis of what has been said above, we may expect such corrections to increase the values given on the ordinates by as much as 50%, but the shapes of the curves should be little affected. Further, the measurements were made over only a limited flight path. Since the time distribution of the electrons must be the same as the time distribution of the x rays, we can estimate that we detect approximately 32% of the electrons. Finally, there are presumably a large number of electrons with energies below 40 keV.

Considerable structure is evident in the yield per fragment of electrons with energies between 40 and 70 keV. A maximum in the yield occurs at mass 108, near the mass of the most probable light fragment. After dropping to zero at mass 130, the yield goes through an inflection at mass 140–145, which is the region of the most probable heavy fragment. The yield then rises to a pronounced maximum around mass 153 and falls off rapidly at higher masses. This peak is very sharp, with a width on the order of 14 mass units at one-half maximum. The ratio of its height to that of the peak at mass 108 is 4.2. The structure changes markedly in going to the next 30-keV group. The

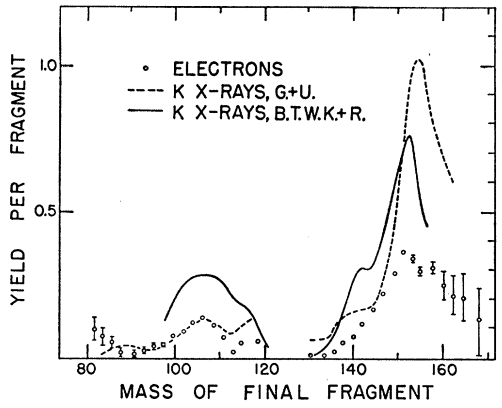

FIG. 12. Yield of electrons summed over all energies as a function of final fragment mass (open circles). The solid curve represents the K x-ray yield data of Bowman and co-workers (Ref. 4) and the dashed curve those of Glendenin and Unik (Ref. 3). The three sets of data represent different time intervals after fission (see text).

inflection at mass 140 is no longer apparent and the peak at higher masses has broadened considerably. Both peaks have shifted to somewhat lower mass numbers while the ratio of the peak heights has dropped to 2.8. The next energy group, encompassing a larger range of 200 keV (to obtain reasonable statistical errors), is quite similar to the previous. The ratio of the peak heights is about 2.4. The highest energy group is completely featureless; the net number of electrons in this range is quite small compared to the gamma-ray background.

In Fig. 12, our results for the yield per fragment of electrons between 40 and 650 keV are plotted together with a schematic representation of the K x-ray yields of Glendenin and Unik (dashed line)[3] and of Bowman, Thompson, Watson, Kapoor, and Rasmussen (solid line).[4]

As can be seen, the electron and x-ray results show the same general features: a small peak near mass 110 and a larger one slightly beyond mass 150. It is difficult to make quantitative comparisons of the yields among the three sets of data. The curve reported by Glendenin and Unik differs in shape and magnitude from that given by Bowman *et al.* Although the time intervals after fission that are sampled differ in the two experiments, it is difficult to understand how Bowman *et al.* could have detected fewer x rays at mass 152 in 50 nsec after fission than Glendenin and Unik detected in 1 nsec. We estimate that about two-thirds of the electrons are emitted outside the timing range of our experiment, that about one-quarter have initial energies below the level of our discriminator, and that about one-third backscatter to deposit an energy in the detector below the discriminator level. Correcting our data at mass 110 (0.135 electrons per fragment) and mass 151 (0.365) we obtain values of 0.81 and 2.19 vacancies, respectively. At mass 110 we estimate that 80% of the transitions convert in the K-electron shell (assuming an average transition energy of 75 keV and equal probabilities of $E2$ and $M1$ radiation).[16,17] Combining this estimate with a value of 0.77 for the K fluorescence yield,[18] we calculate that there should be 0.50 K x rays per fission at mass 110. Similarly, with an estimate of 63% conversion in the K shell and a fluorescence yield of 0.90, we obtain 1.24 K x rays per fission at mass 151. Although these values are higher than those reported, the ratio of the value at mass 151 to that at 110 (2.5) is the same as found by Bowman *et al.*, but considerably different from that found by Glendenin and Unik (≈ 7). The correction factors we have used in making these comparisons are quite uncertain; in gross magnitude and shape there is general agreement among the three sets of data.

IV. DISCUSSION

A. Multipolarities

The results obtained on the emission times of the x rays allow us to draw reasonably unambiguous conclusions about the multipolarities of the converted transitions. Although the range of half-lives we have measured in the x-ray experiment is from less than 10^{-11} sec to 2.5×10^{-9} sec, the spectrum of electrons represents those emitted in the time interval 10^{-10} to 1.5×10^{-9} sec after fission. The electron data of Fig. 6 show that most of the transitions occurring in this interval have energies between 30 and 200 keV. In Fig. 13 we have outlined the approximate half-life and energy area delimited in our experiment. In addition, we have plotted the known half-lives and energies for transitions of various multipolarities in the mass region 100–170.[19] No transitions of multipolarity higher than $E2$ or $M1$ fall within the range of this figure. The locus of $E2$ lifetimes crosses one corner of the range of results obtained in our experiment; points for $M1$-$E2$ mixtures are found throughout this range. We conclude that dipole transitions must contribute strongly and that probably most of the transitions we have observed are $M1$ or $M1$-$E2$ mixtures. The occurrence of $E1$ transitions cannot be excluded, but the total number of electrons emitted and the range of lifetimes observed do not seem to be consistent with a large contribution from $E1$ transitions. These conclusions are consistent with the assumptions made by Glendenin and Griffin[12] in fitting the data they obtained on the yield of K x rays as a function of x-ray energy.

[16] L. A. Sliv and I. M. Band, in *Alpha-, Beta-, and Gamma-Ray Spectroscopy*, edited by K. Siegbahn (North-Holland Publishing Company, Amsterdam, 1965), Vol. II, p. 1639.

[17] M. E. Rose, *Internal Conversion Coefficients* (Interscience Publishers, Inc., New York, 1958).

[18] I. Bergström and C. Nordling, in *Alpha-, Beta-, and Gamma-Ray Spectroscopy*, edited by K. Siegbahn (North-Holland Publishing Company, Amsterdam, 1965), Vol. II, p. 1523.

[19] J. Lindskog, T. Sundström, and P. S. Sparrman, in *Alpha-, Beta-, and Gamma-Ray Spectroscopy*, edited by K. Siegbahn (North-Holland Publishing Company, Amsterdam, 1965), Vol. II, p. 1599.

Using these conclusions we can make some estimate of the transition-energy spectrum (as opposed to the electron spectrum). Assuming $Z=50$ for an average fission fragment and equal probability for $E2$ and $M1$ transitions we can obtain conversion coefficients for K, L, and M conversion.[16,17] Combining these with an assumed flat transition spectrum from 0 to 500 keV, we calculate the dashed curve of Fig. 6 (arbitrarily normalized in height). From a comparison of this curve with the data we conclude that the exponential decrease in electrons detected as a function of energy is due to the more or less exponential decrease in conversion coefficients with transition energy. This conclusion is not sensitive to the $M1$-$E2$ mixing ratio assumed. The decrease in gamma-ray intensity[20] below 150 keV that has been observed is consistent with these conclusions.

B. Electron Spectra

The spectra shown in Fig. 9 are from nuclei in the mass region where stable deformations are well-known.[21] Since de-excitation through rotational bands of the fragments is likely to be important, one may hope to correlate some of the peaks with rotational transitions. Data on the energy levels of the neutron-rich nuclei produced in fission have heretofore not been available; in order to attempt such a correlation it is necessary to estimate the transition energies by extrapolation from data on neighboring nuclei.[22] For even-even nuclei in the region of the heavy-fragment masses, we have extrapolated along lines of constant neutron number to even-even nuclei in the region of most probable charge.[3,4] The results are expected to be fairly accurate in this region because of the slow rate of change of level energy with atomic number and the small extrapolation required (1 to 4 mass units). For all four even-even nuclei between masses 150 and 164, the energies of the 2+, 4+, and 6+ levels are very close to 74, 245, and 505 keV, respectively. The fact that these energies are common to these nuclei together with the simple de-excitation pattern characteristic of these nuclei make it reasonable to suppose that conversion electrons from their low-energy transitions may be prominent among the larger unresolved distribution of lines from odd-mass nuclei that probably contribute most of the intensity observed in the electron spectra. For a 74-keV transition, the K- and L-conversion electrons have energies of 25 ± 5 and 66 ± 1 keV and conversion coefficients of 2 and 3.5, respectively.[16,17] The K-conversion line is at the discriminator setting and is, therefore, too low to be observed. The spectra of Fig. 9, which include

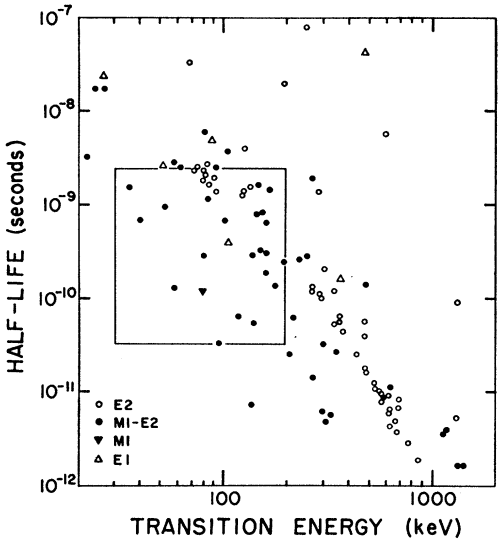

FIG. 13. Half-lives and energies of transitions studied in this work compared with half-lives and energies of other transitions. The solid line indicates the approximate range of half-lives and energies studied by us. The points represent experimental values for transitions of the indicated multipolarities (Ref. 19).

part of this mass range, indeed show peaks between 63 and 68 keV. The expected electron energies from the 171-keV transitions between the 4+ levels (at 245 keV) and the 2+ levels (at 74 keV) are 122 ± 5 and 163 ± 1 keV with conversion coefficients of about 0.37 and 0.17, respectively. In each of the spectra labeled 153, 155, and 158 strong lines are evident at these energies with relative intensities consistent with the conversion coefficients. It does not require too great a stretch of the imagination to see evidence for the 211 ± 5 keV electrons corresponding to K conversion of the 6+ to 4+ transition. In Fig. 8 two strong lines at 77 and 168 keV are obvious for mass curves 145 and 142. One can, by assigning these lines and other less obvious ones appropriately, make a case for the observation of the lower members of a rotational band; the case is not solidly based however.

We consider next the spectra associated with the light-fragment peak (Fig. 7). Johansson has seen evidence for transitions of about 130 and 300 keV in the mass 110 region.[23] He asserts that 130 keV is approximately the energy of the transition between the 2+ and ground states and that 300 keV is then the energy of the 4+ to 2+ transition. Our data in this mass region show electron lines at about 225 and 80 keV, corresponding to transitions of about 245 and 100 keV converted in the K shell. These energies are not far from those reported by Johansson and the energy ratio is in reasonable agreement with what one would expect for a rotor with a constant moment of inertia. Closer inspection of the data indicates, however, that the maximum yield of the 225-keV electrons occurs at about

[20] V. V. Skliarevskii, D. E. Fomenko, and E. P. Stepanov, Zh. Eksperim. i Teor. Fiz. **32**, 256 (1957). [English transl.: Soviet Phys.—JETP **5**, 220 (1957)].

[21] O. Nathan and S. G. Nilsson, in *Alpha-, Beta-, and Gamma-Ray Spectroscopy*, edited by K. Siegbahn (North-Holland Publishing Company, Amsterdam, 1965), Vol. I, p. 601.

[22] *Nuclear Data Sheets*, Compiled by K. Way *et al.* (Printing and Publishing Office National Academy of Sciences—National Research Council Washington, D. C.).

[23] S. A. E. Johansson, Nucl. Phys. **64**, 147 (1965).

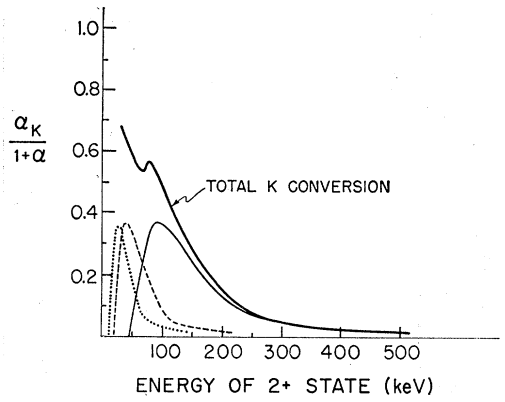

FIG. 14. K conversion during the de-excitation of a rotational band of an even-even nucleus of $Z=60$ as a function of the energy of the lowest 2+ state. The light solid line represents conversion of the 2+ to 0+ transition, the dashed line conversion of the 4+ to 2+, and the dotted line conversion of the 6+ to 4+. The heavy solid line represents the sum of the three.

mass 110, whereas the yield of the lower energy electrons peaks near mass 104. We, therefore, cannot say there is any definite evidence from our data for rotational transitions in these nuclei.

C. Electron Yield as a Function of Fragment Mass

The electron yield per fragment as a function of fragment mass shows strong maxima near masses 110 and 150 together with a vanishing yield at mass 130. Because of the rapid decrease of internal conversion coefficients with increasing transition energy, we associate a high electron yield with a high multiplicity of low-energy transitions and a low electron yield with a low multiplicity of such transitions. As has been noted by others,[3,4] the sharp rise in the yield of K x rays just above mass 140 corresponds to the onset of a region of stable nuclear deformation.[21] Nuclei in this region are characterized by well-defined rotational bands of closely spaced levels and hence highly converted transitions. Similarly, the low yield near mass 130 may be associated with the closed-shell configuration 50 protons and 82 neutrons. Levels in this region are expected to be widely spaced and transitions to be of too high an energy to be appreciably converted. For the mass region 100–110, where we observe a maximum in the electron yield Johansson[23] proposes the existence of stable nuclear deformations. The most probable Z for fragments of mass 110 is about 45, halfway between the closed subshell at $Z=40$ and the closed shell at $Z=50$. Similarly, the most probable neutron number is 65, halfway between the closed shells at $N=50$ and 82. In addition to the arguments presented by Johansson for the existence of deformations, we note that the energies of the lowest 2+ states of the molybdenum, ruthenium, and palladium isotopes drop markedly and that the $B(E2)$ values (relative to the single-particle estimate) increase as the neutron-to-proton ratio increases.[21] These trends may indicate that the neutron-rich isotopes of these elements have stable deformations and de-excite through several low-energy, highly converted transitions.

It should be noted that the existence of closely spaced levels is not a sufficient condition for the production of a relatively large number of conversion electrons. It is necessary that the fragments be formed with enough angular momentum so that de-excitation takes place through a sequence of these levels. A large nuclear spin may easily be produced in a deformed fragment if the scission configuration is not axially symmetric. This may not be the case for a fragment that is spherical at scission. Thus, there are possibly two reasons for low electron yield from fragments in the vicinity of closed shells: low spin and large transition energy.

Although these arguments account for the major features of the yield curves, there are several questions left unanswered. The most striking of these is why does the yield of electrons fall so sharply beyond mass 153, while the region of stable deformation extends to about mass 180. In addition, one would like to account for the inflection seen in the low-energy electron data near mass 140 and for the changes in positions and widths of the peaks with increasing electron energy.

Glendenin and Unik,[3] following a suggestion made by Vandenbosch,[24] have explored the possibility that the major source of K x rays near mass 150 is converted transitions of energy only slightly greater than the K-electron binding energy. As the nuclear mass and charge increase, the difference between the transition energy and the K-shell binding energy decreases and the probability of conversion in the K shell decreases. They reached no conclusion concerning the validity of this suggestion. It is clear, however, that this hypothesis cannot explain the turnover in electron yield. First, from the data of Fig. 11, we see that this phenomenon is occurring for transitions with up to 100 keV in excess of the binding energy of the converted electrons. Second, although K-shell conversion becomes improbable at low-transition energy, the probability for L and M conversion is close to 1; even if such an explanation were correct for the yield of K-shell vacancies, it would not apply to the total yield of vacancies, which is the quantity measured in our electron experiments. Finally, a decrease in the yield of K-shell vacancies above mass about 153 could occur as a result of the suggested effect only if de-excitation does not take place through the higher members of the rotational bands. As the energy of the last transition in a rotational band approaches the K-electron binding energy, the increased conversion of the higher members more than makes up for the loss. This effect is illustrated for an even-even nucleus of $Z=60$ in Fig. 14, where we have plotted the yield of K-shell vacancies during de-excitation of a rotational band as a function of the energy of the 2+ state.

[24] R. Vandenbosch, in *Physics and Chemistry of Fission* (International Atomic Energy Agency, Vienna, 1965), Vol. I, p. 399.

Glendenin and Unik[3] have considered contributions to the conversion process from the different nuclear types and have concluded that the odd-mass and odd-odd nuclei will contribute more to the yield of vacancies than do the even-even nuclei. In addition, they have noted the abnormally high moments of inertia of nuclei in the mass 150 region. Pursuing this point, we note that the high vacancy yields occur for fission fragments with neutron numbers 89 to 97 and proton numbers close to 61. Prominent among the low-lying levels of nuclei with these neutron numbers are the $(532)\frac{3}{2}-$, $(651)\frac{3}{2}+$, and $(642)\frac{5}{2}+$ single-particle states, and with this proton number the $(532)\frac{5}{2}-$ state. Nuclei with the odd nucleon in these states have moments of inertia almost twice the values expected from the neighboring even-even nuclei.[25] For higher neutron and proton numbers moments of inertia are normal. It is possible that the high yield just beyond mass 150 is connected with the particularly small level spacings associated with the large moments of inertia. We have, however, not been able to account for the decrease in yield beyond mass 153 using reasonable assumptions about the number of transitions and the relative amounts of $M1$ and $E2$ conversion.

Other conceivable explanations for the drop in yield beyond mass 153 are that the fission fragments are formed with no excitation energy or that there are no closely spaced transitions in these nuclei. The first of these suppositions is inconsistent with other data about the fission process; the second is inconsistent with the general systematics of nuclear energy levels in this region. It may also be possible that the character of the levels at high excitation changes in such a way that the nucleus reaches the ground state via high-energy, unconverted transitions.

Finally, we consider the possibility that the decrease above mass 153 and perhaps some other features of the yield curve as well may be due to a dependence of the spin imparted to a fragment on the nature of the partner fragment. It may be noted that as the heavy-fragment mass increases beyond 153, the partner mass is decreasing toward the closed shell at $N=50$. It is possible that closed shell, spherical nuclei, which cannot themselves receive spin by a simple Coulomb interaction, may be less effective in imparting spin to their deformed partners than are deformed nuclei. Hoffman[26] has estimated that a spheroidal fragment produces about 10% more angular momentum than does a spherical one in some given spheroidal partner. Hence, one might expect a decrease in the spin of both fragments as the light-fragment mass approaches the closed shell at $N=50$. Furthermore, any spin given to the deformed fragment by a spherical one must be matched by orbital angular momentum between the two fragments; such a division might be inhibited by the centrifugal barrier.

[25] J. P. Davidson, Rev. Mod. Phys. **37**, 105 (1965).
[26] M. M. Hoffman, Phys. Rev. **133**, B714 (1964).

The results of Hohmann[27] on K x rays emitted in the fission of U^{236} may be considered in the light of these arguments. If the x-ray yield per fragment of a given mass is taken to be independent of partner mass then the curves of Fig. 12 together with the total x-ray yield from Cf^{252} of 0.57 may be used to calculate the total yield of K x rays produced in the fission of U^{236}. This is found to be about 0.33 per fission, to be compared with 0.2 ± 0.06 reported by Hohmann. If, on the other hand, the argument presented above is valid, the yield of electrons or K x rays from U^{236} fission should not show the strong peak at mass 153, since fragments of this mass will be paired with closed-shell partners ($Z\cong32$, $N\cong49$). From the difference in mass and number of neutrons emitted between Cf^{252} and U^{336} we estimate that a sharp decrease corresponding to that seen at mass 153 for Cf^{252} should be seen at about mass 139 for U^{236}. If we assume that the yield per fragment above mass 140 is zero and that below 140 it is the same for U^{236} as it is for Cf^{252}, then we obtain 0.18 for the yield of K x rays per fission in U^{236}.

It should be pointed out, however, that this explanation does not seem to be in accord with the reported data on number and average energy of gamma rays from U^{236} and Cf^{252} fission. It is expected that high angular momentum in the fission fragments will be associated with a relatively low probability for neutron emission and with a large energy dissipated in gamma rays and a high multiplicity of gamma rays. On the basis of the proposed explanation we would expect that if either fragment is a closed-shell nucleus then there will be low angular momentum and hence a low multiplicity and energy of gamma rays. The data of Maier-Leibnitz, Schmitt, and Armbruster[28] indicate, however, that the average energy emitted as gamma rays per fission is more or less independent of mass ratio. Furthermore, although their results show a lower than average energy from nuclei near closed shells, the partner nuclei yield a higher than average energy. The work of Rau[29] indicates that the multiplicity of gamma rays is not especially low if one of the fragments is a closed-shell nucleus. Finally, Johansson's results[13] from Cf^{252} show a high yield of gamma rays around mass 120, which, as the partner of fragments with masses near 132, would be expected to have a low yield. Similarly, there is no decrease in gamma-ray yield beyond mass 153 corresponding to the decrease seen in the electron yield.

ACKNOWLEDGMENTS

The Cf^{252} from which the sources were prepared was obtained from the Chemistry Division of the Lawrence Radiation Laboratory, to whom we are grateful. We

[27] H. Hohmann, Z. Physik **172**, 143 (1963).
[28] H. Maier-Leibnitz, H. W. Schmitt, and P. Armbruster, unpublished results quoted in Ref. 2.
[29] F. E. W. Rau, Ann. Physik **10**, 252 (1963).

have benefited from discussions with Professor Robert A. Naumann and Dr. J. S. Evans.

APPENDIX: MASS CALIBRATION AND DISPERSION CORRECTION

The questions of mass calibration and mass dispersion are closely intertwined and it is impossible to consider one without the other. We discuss in this section the steps that were taken to correct for mass dispersion and to determine the mass calibration.

The fragment masses are derived from the fragment kinetic energies. If no neutrons are emitted, conservation of momentum gives the mass of the fragments. Terrell has pointed out that neutron emission has two effects.[30] First, it introduces a dispersion in mass because of variation in neutron number, direction, and energy; this dispersion is estimated by Terrell to increase the variance of the mass distribution by 2.8 mass units squared. Second, there is a shift of the apparent mass determined in this way from the prompt fragment mass by as much as one mass unit due to the correlation between the average number of neutrons emitted and the mass of the fragment.

Instrumental effects give rise to additional dispersion and to nonproportionality between the pulse-height ratio and the fragment mass. Semiconductor detector resolution for bromine and iodine ions has been measured to be 1 to 2 MeV (full width at half-maximum) over a wide range of energies.[7] For this effect we may estimate an increase in variance of less than 1 mass unit squared. The summing and dividing circuitry introduces further dispersion. Shepherd's grouping correction is about 0.5 mass unit squared.[30]

Altogether, we may expect the experimental data to have a variance that is at least 4 mass units squared greater than the true variance. We have estimated the actual value of this increase from the number of mass channels over which a peak in the electron spectrum is distributed. The value of the root-mean-square deviation from the average for several such peaks is about 1 channel, or 2.3 mass units, corresponding to an increase in variance of 5.3 mass units squared, in reasonable agreement with expectations. The first step in processing the results was to remove this much dispersion from the data using a combined smoothing and resolving function suggested by Terrell.[30]

Because of pulse-height defect, the pulse heights corresponding to particular fission fragments are not proportional to the energies of those fragments.[7] The data available indicate, however, that the pulse height varies linearly with fragment mass and energy.[7–9] In this case, the pulse-height ratio $X_B/(X_A+X_B)$ varies linearly with the energy ratio $E_B/(E_A+E_B)$.

The mass calibration was done as follows: The data of Fraser, Milton, Bowman, and Thompson[31] were adjusted for the effects of correlated neutron emission to give a curve representing yield versus calculated mass (M^c). Calculated mass is defined by the expression.

$$M_A{}^c=252[E_B/(E_A+E_B)]$$

in which E_A and E_B are, as above, the kinetic energies after neutron emission. The difference between the calculated mass ($M_A{}^c$) and the mass before neutron emission (M_A) is

$$M_A{}^c-M_A=(M_B\nu_A-M_A\nu_B)/252,$$

where ν_A and ν_B are the numbers of neutrons emitted from fragments A and B. In making this adjustment, we used values of ν given by Terrell.[30]

From the curve of yield versus calculated mass so constructed, five points were chosen for the mass calibration: the mass numbers corresponding to the two maxima and the one minimum and the midpoints at half-maximum of the two peaks. The channel numbers corresponding to the same points in binary mass yield data were ascertained. A least-squares fit gave the relationship between calculated mass and channel number. This was readjusted for the effects of correlated neutrons to give the relationship between mass before neutron emission and channel number. As a test of the self-consistency of this process, we have compared in Fig. 15 the binary mass yield determined in our experiments with that reported by Fraser *et al.*[31] The agreement, in terms of peak-to-valley ratio, width of peaks, and position of peaks is quite satisfactory.

Because the x-ray and electron emission occurs from the fragments after neutron emission we have subtracted from the prompt masses the number of neutrons emitted to give a relationship between final mass and channel.

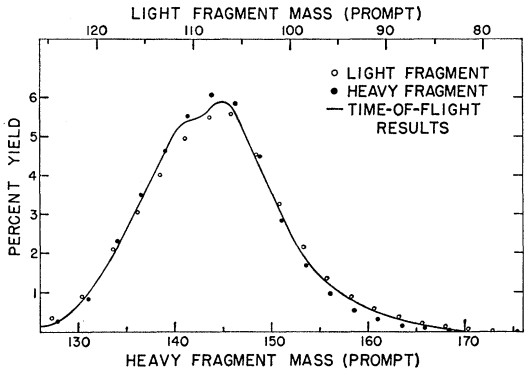

FIG. 15. Mass-yield curve determined using the adder-divider circuit and the calibration method described in the Appendix. The solid line represents the time-of-flight results given in Ref. 31.

[30] J. Terrell, Phys. Rev. **127**, 880 (1962).

[31] J. S. Fraser, J. C. D. Milton, H. R. Bowman, and S. G. Thompson, Can. J. Phys. **41**, 2080 (1963).